Induced Long-Range Attractive Potentials of Human Serum Albumin by Ligand Binding

Takaaki Sato,[1,2,*] Teruyuki Komatsu,[2,3] Akito Nakagawa,[2] and Eishun Tsuchida[2,†]

[1]*Division of Pure and Applied Physics, Faculty of Science and Engineering, Waseda University, 3-4-1 Okubo, Shinjuku-ku, Tokyo 169-8555, Japan*

[2]*Advanced Research Institute for Science and Engineering, Waseda University, 3-4-1 Okubo, Shinjuku-ku, Tokyo 169-8555, Japan*

[3]*PRESTO, Japan Science and Technology Agency (JST), 4-1-8 Honcho, Kawaguchi-shi, Saitama 332-0012, Japan*

(Received 9 July 2006; published 15 May 2007)

Small-angle x-ray scattering and dielectric spectroscopy investigation on the solutions of recombinant human serum albumin and its heme hybrid revealed that heme incorporation induces a specific long-range attractive potential between protein molecules. This is evidenced by the enhanced forward intensity upon heme binding, despite no hindrance to rotatory Brownian motion, unbiased colloid osmotic pressure, and discontiguous nearest-neighbor distance, confirming monodispersity of the proteins. The heme-induced potential may play a trigger role in recognition of the ligand-filled human serum albumins in the circulatory system.

DOI: 10.1103/PhysRevLett.98.208101 PACS numbers: 87.14.Ee, 61.10.Eq, 83.80.Lz

Human serum albumin (HSA) is the most abundant plasma protein in our bloodstream, whose primary functions are transportation of hydrophobic molecules and adjustment of colloid osmotic pressure (COP) of blood [1]. Owing to its nonspecific ligand-binding capability, HSA has served many potential medical applications. Information on HSA-ligand interactions and their structural basis have recently been available by x-ray crystal structure analysis [2–5]. Such approaches have provided a structural foundation to create functional protein-ligand complexes. One of the promising materials is the rHSA-heme hybrid that can transport oxygen as hemoglobin does [6–9]. The material is currently investigated in preclinical tests as an artificial blood substitute [8]. Recent manifold interests in protein crystallography, critical phenomena, and disease processes have attracted increasing attention to interparticle interactions in globular protein solutions [10–15]. However, the fundamental problems like an influence of the ligand-binding upon protein-protein interactions remain elusive.

We investigated solutions of recombinant HSA (rHSA) (MW 66.5 kDa) and its heme hybrid [rHSA-heme; rHSA incorporating four iron-porphyrins (synthetic hemes)] [7]. Using small-angle x-ray scattering (SAXS), we scrutinized spatial correlations of these proteins in a 0.15M phosphate buffer saline (PBS) solution to fulfil ionic strength and pH close to physiological conditions and those in water to minimize ionic strength. The PBS solution of rHSA-heme (heme/rHSA = 4, mol/mol) was prepared according to our previously reported procedures [7]. The deionization of the protein sample was performed by several cycles of centrifugation/dilution with pure water using a Millipore Amicon Ultra to give aqueous solution of rHSA-heme. The solutions were passed through a 0.22 μm filter before all measurements. The deep red-colored, transparent solution of rHSA-heme can long be stored without precipitation or liquid-liquid phase separation. It has been confirmed that isoelectric point (pI), solution viscosity, and COP for rHSA-heme under the physiological environment are identical to those of rHSA.

All SAXS experiments were carried out by using a SAXSess camera (Anton Paar) in the q range of 0.072–5 nm^{-1}. A model-independent collimation-correction procedure was made via an indirect Fourier transformation (IFT) routine and/or based on a Lake algorithm. We also performed dielectric relaxation spectroscopy (DRS) experiments on aqueous rHSA and rHSA-heme solutions in the frequency range of $0.0005 \leq \nu/\mathrm{GHz} \leq 20$ using time domain reflectometry [16].

Figure 1 shows SAXS experiments on a concentration series of rHSA in PBS solution at 25 °C. The normalized scattered intensities $I(q)/c$, where $I(q)$ is the scattered intensity at scattering vector q and c the protein concentration, exhibit a decreasing forward intensity $I(q \to 0)/c$ with increasing c [Fig. 1(a)]. HSA carries a net negative charge of about 18 electronic charges at pH 7.4 [1]. Since the long-range electrostatic repulsion between rHSAs is efficiently screened in the PBS solutions, the suppressed forward intensity is mainly attributed to the decreased osmotic compressibility due to the increased particle number density. Lowering c results in the convergence of $I(q)/c$ to the intrinsic form factor $P(q)$ of rHSA, achieving the structure factor $S(q) \sim 1 (c \to 0)$.

The pair-distance distribution functions $p(r)$ of rHSA [Fig. 1(b)] in solution are obtained using generalized indirect Fourier transformation (GIFT) technique [17], for which we approximated $S(q)$ assuming a Yukawa potential and the Rogers-Young closure. The procedure confirms the existence of oblatelike particles having the maximum diameter of $D_{\max} \sim 8.0$–8.5 nm at all c. All features of $p(r)$ highly resemble those calculated from x-ray crystallography data on HSA (Protein Data Bank code 1UOR) [3].

Figure 2(a) presents variation of $I(q)$ of rHSA solutions, depending on the presence and absence of the heme incorporation and ionic strength of solvents. The more pronounced decrease of the forward intensity and the sig-

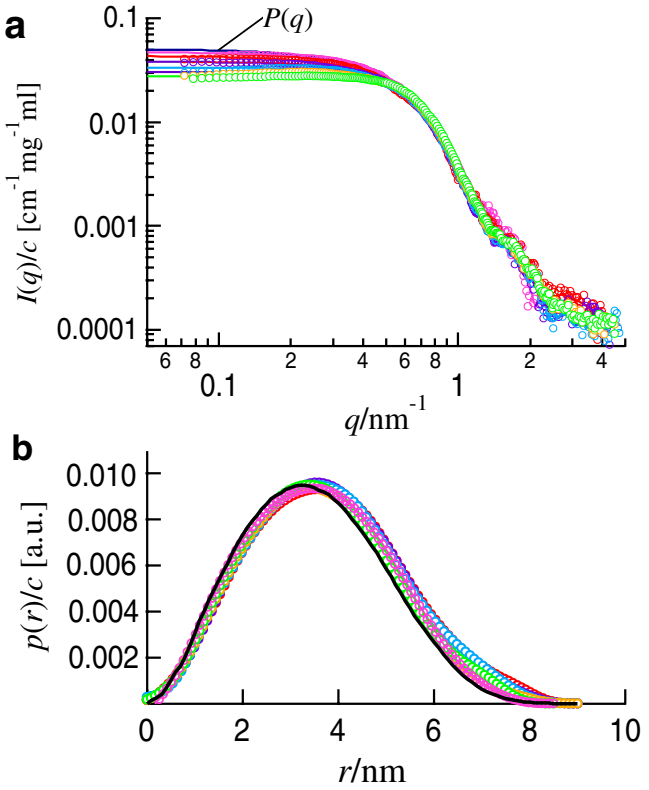

FIG. 1 (color online). (a) The normalized x-ray scattered intensities, $I(q)/c$, and (b) the pair-distance distribution functions, $p(r)$, of rHSA in 0.15M PBS solutions in $3.0 \leq c/\mathrm{mg\,ml^{-1}} \leq 50$. The black solid curve shown in (b) represents $p(r)$ calculated from the crystallography data on HSA [3].

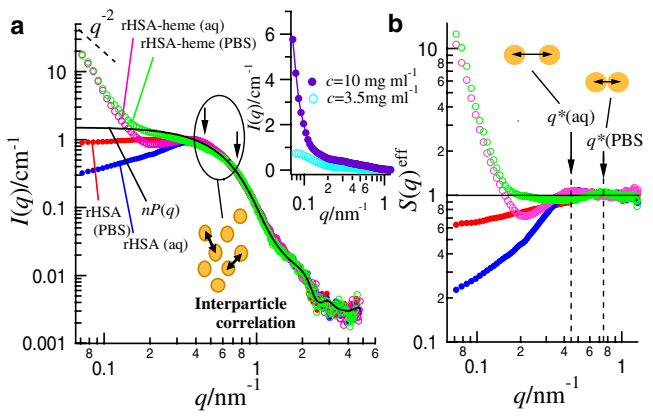

FIG. 2 (color online). (a) Variation of $I(q)$ and (b) the effective structure factors $S^{\mathrm{eff}}(q)$ for rHSA and rHSA-heme in aqueous and 0.15M PBS solutions of a fixed concentration $c = 30\ \mathrm{mg\,ml^{-1}}$. In the inset, the low-$q$ intensities for $c = 3.5\ \mathrm{mg\,ml^{-1}}$ and $c = 10\ \mathrm{mg\ ml^{-1}}$ are compared. Arrows on $S^{\mathrm{eff}}(q)$ highlight the monomer-monomer correlation peak positions q^*.

nificant low-q shift of the monomer-monomer correlation peak position for aqueous rHSA reflect the only weakly screened, thus stronger electrostatic repulsions between the rHSA molecules. Importantly, we observed that heme-incorporated samples exhibit an enhanced forward intensity, which indicates that heme incorporation significantly enhances particle density fluctuations on a large length scale.

Further insights into the spatial correlations between the proteins are gained from the effective structure factors $S^{\mathrm{eff}}(q)$ [11] [Fig. 2(b)]. We extracted $S^{\mathrm{eff}}(q)$ by dividing $I(q)/c$ by $P(q)$ obtained from a dilute rHSA PBS solution. We confirmed that for rHSA-heme, lowering c from 10 to 3.5 $\mathrm{mg\,ml^{-1}}$, leads to a significantly weaker relative low-q intensity, $I(q)/c$, as shown in Fig. 2. In terms of $S^{\mathrm{eff}}(q)$, rHSA under physiological condition still preserves the nature of a repulsively interacting charged colloid but behaves nearly as a hard sphere. If we apply a Yukawa potential model to $S^{\mathrm{eff}}(q)$ with *a priori* input of the solvent ionic strength, the effective protein charge of 18 ± 2 is obtained, being consistent with Ref. [1]. Solutions of rHSA-heme exhibit a similar low-q upturn in $S^{\mathrm{eff}}(q)$, independent of ionic strength. The observation suggests the emergence of a long-range attractive interaction [12,13] between the heme-incorporated rHSA molecules. However, this assignment is only valid when the monodispersity assumption of the protein is fulfilled. In the following, we carefully verify this interpretation, providing convincing evidence for monodispersity of rHSA-heme.

The peak in $S^{\mathrm{eff}}(q)$ arises from protein-protein positional correlations [Fig. 2(b)]. The mean nearest-neighbor distance d^* among the proteins is approximated as $\sim 2\pi/q^*$, where q^* is the scattering vector corresponding to the peak position of $S^{\mathrm{eff}}(q)$. Importantly, q^* is essentially independent before and after heme binding, but it simply depends on the solvent ionic strength related to the screening of the long-range electrostatic repulsion. In Fig. 3, we display a concentration series of $S^{\mathrm{eff}}(q)$ for rHSA and rHSA-heme solutions at different ionic strength. For aqueous rHSA and rHSA-heme, increasing c shifts q^* to higher values, holding a relation $q^* \propto n^{1/3}$ [Fig. 3(e)], where n is the particle number density. The finding clearly shows that both aqueous rHSA and rHSA-heme exhibit a typical feature of charged colloids at low ionic strength, maximizing d^*.

The identical COP (18 mmHg at $c = 50\ \mathrm{mg\ ml^{-1}}$) between the solutions of rHSA-heme and rHSA despite a half value for covalently dimerized rHSA at the same volume fraction [6] also rules out irreversible aggregate formation in rHSA-heme solutions. A simple model calculation demonstrates that a compact aggregate having several tens of aggregation number can never explain the observed low-q feature. No further enhancement of the low-q rise upon screening of the electrostatic repulsion excludes a strong short-range attraction as its origin.

Figure 4 presents complex dielectric spectra of rHSA and rHSA-heme solutions at various c. The relaxation time $\tau_{\mathrm{water}} \sim 8.3$ ps for the high-frequency process common for all solutions reflects the time scale of cooperative rearrangement of the hydrogen-bond network of bulk water [16,18,19]. Besides, the low-frequency relaxation, as-

signed to the rotational diffusion of the proteins [19,20], gives an excellent measure of dimer or higher aggregate formation. The identical relaxation times before and after heme binding, $\tau_{\mathrm{rHSA}} \sim 52$–$58$ ns, provides identical effective molar volume for rHSA and rHSA-heme, $V^{\mathrm{eff}} = 4.7 \times 10^4\ \mathrm{cm^3\,mol^{-1}}$ $(c \rightarrow 0)$, according to the Stokes-Einstein-Debye equation, which is very close to the anticipated value of $4.9 \times 10^4\ \mathrm{cm^3\,mol^{-1}}$ from the molecular mass and specific volume of HSA. This reveals that the freedom of the rotational diffusive motion of the protein is not significantly affected by the heme incorporation.

We point out that in contrast to HSA, well-investigated aqueous lysozyme solutions [11–14,21,22] are already in aggregation regime; even at very low ionic strength, most of lysozyme molecules stick together due to its highly adhesive nature, which is demonstrated by the appearance of the low-q subpeak in $S^{\mathrm{eff}}(q)$ and d^* coinciding with the diameter of the protein molecule. Although there arose a controversy as to whether the low-q rise for lysozyme solutions is due to a long-range attraction (LRA) [13,21] or large aggregate formation [22], as for rHSA-heme, the simultaneous observations of the low-q rise in $S^{\mathrm{eff}}(q)$ with a host of evidence for monodispersity of the protein, such as d^* far exceeding the contact distance, no additional frictional force on the rotational diffusive motions, identical molecular volume with rHSA, and unbiased COP, provide a plausible argument for the emergence of a LRA. Note that any kind of protein aggregation requires the direct contact between the monomers. Generally, when the repulsion is so strong as to make the particles apart, the low-q rise can be explained only by a LRA [12].

The theoretical $S(q)$ analysis based on a two Yukawa potential model [13] has shown that the relatively longer attraction range than the repulsion one is necessary to produce the so-called zero-q peak in $S(q)$. The more pronounced low-q decrease in $S^{\mathrm{eff}}(q)$ for aqueous rHSA is clearly taken over by the deeper dip in $S^{\mathrm{eff}}(q)$ for aqueous rHSA-heme, which indicates that the electrostatic repulsion is still active in rHSA-heme solutions and the attraction range is greater than the range of the weakly screened electrostatic repulsion.

For further quantitative description, we tested a two Yukawa model [12,13] for $S^{\mathrm{eff}}(q)$ of rHSA-heme. When the attraction range is very long, the model produces a downward convex low-q rise and a huge zero-q intensity reaching more than $\sim$1000 even at small c. However, $S(q)$ starts to rise at $q \leq 0.1\ \mathrm{nm^{-1}}$, whereas we observed the onset around $q = 0.2\ \mathrm{nm^{-1}}$. The real expression for a LRA and its potential shape are still not very clear, but the formalism of the potential should significantly affect the low-q shape of $S(q)$. If the system exhibits more slowly decaying attractive potential than the Yukawa decay at small-r, the onset of the low-q rise is expected to shift to higher-q values than that predicted by the Yukawa LRA model.

It is important to recognize that isotropic interaction is not self-evident for any kind of protein system because proteins have irregular shape and inhomogeneously distributed patches by nature. However, until now, almost all experimental and theoretical works on the interactions proteins have been performed based on mean spherical approximation (MSA) and an isotropic interaction assumption [10–15,23]. The recent theoretical work of Bianchi *et al.* [24] revealed that particles interacting with an anisotropic attractive potential can enhance anomalous density fluctuations or gel-network formation even at very low volume fractions. This also implies that anisotropic potentials caused by a site-specific interaction or inhomogeneous distributions of charge or hydrophobic patches may generate unexpectedly drastic effects on the spatial correlations of proteins, where the inherent limitation of small-angle scattering technique lies in the fact that such anisotropic interactions are reduced into one-dimensional $S(q)$. Nevertheless, carefully confirmed monodispersity of rHSA-heme leads us to conclude that our present interpretation based on a LRA is still broadly correct, even if the actual situation is much more complicated, where anisotropic interactions may affect the spatial correlation of the proteins.

Compared to the well-developed short-range attraction and long-range electrostatic repulsion [11,13,23], the general understanding of a LRA of proteins in solution

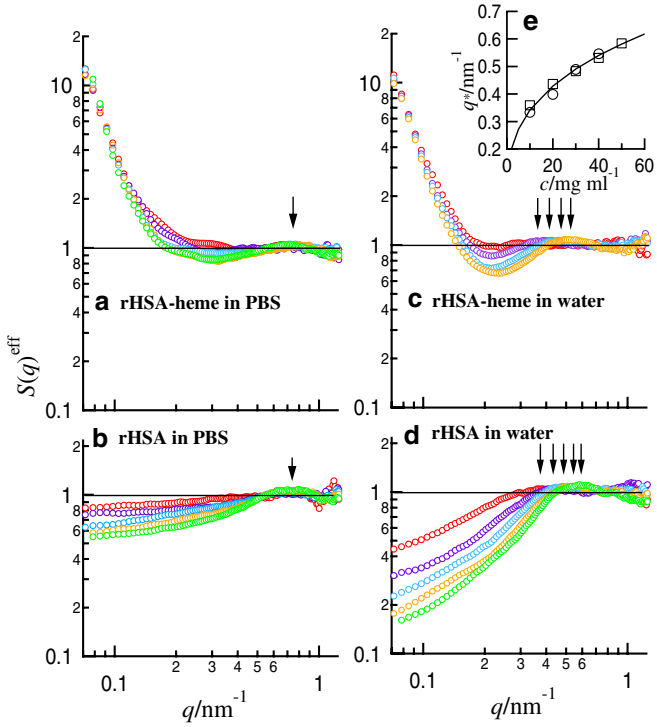

FIG. 3 (color online). Effects of concentration, ionic strength, and heme binding on $S^{\mathrm{eff}}(q)$. (a) rHSA-heme and (b) rHSA in 0.15M PBS solutions and (c) rHSA-heme and (d) rHSA in aqueous solutions in $10 \leq c/\mathrm{mg\,ml^{-1}} \leq 50$ (an increment of 10 $\mathrm{mg\,ml^{-1}}$). (e) The protein-protein correlation peak position q^* in $S^{\mathrm{eff}}(q)$ for aqueous rHSA (□) and rHSA-heme (○) as a function of c.

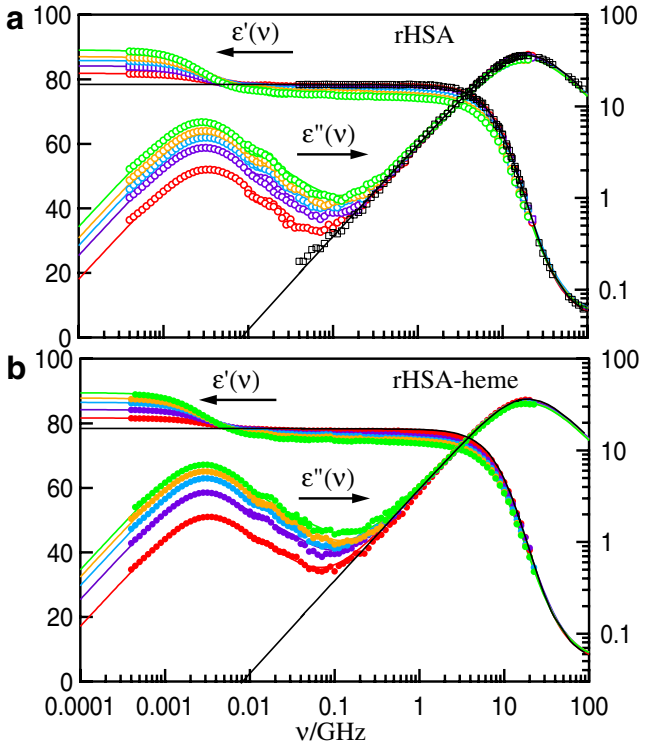

FIG. 4 (color online). Complex dielectric spectra of aqueous solutions of (a) rHSA and (b) rHSA-heme in $10 \leq c/\mathrm{mg\,ml^{-1}} \leq 50$ (an increment of 10 mg ml^{-1} from the bottom) at 25 °C.

[12,13,15] is at an incipient stage. Judging from unbiased $p\mathrm{I}(= 4.9)$ and polarization fluctuation amplitudes for rHSA-heme, net charges and their distributions are unlikely to be modified by heme binding, whereas how the occupation of the ligand-binding site allosterically affects the electrostatic interaction of the protein is unclear. The physical origin of a LRA might be entoropic driven, possibly due to modulated hydrophobic patches and their inhomogeneous distributions.

HSA binds heme; the rHSA-heme hybrid takes advantage of this naturally occurring process. In the human body, heme released from methemoglobin is immediately captured by hemopexin or HSA acting as scavengers, and it is efficiently transported to the liver for methabolism [25,26]. Since the emergence of the collective nature of HSAs while preserving the monodispersity could be an efficient way to give the ligand-filled HSA molecules a sort of marker, our data suggest that the heme-bound or -unbound HSAs may be recognized in the bloodstream in terms of the presence and absence of the LRA. Therefore, the optimization of the interparticle potential will be a key to the control of distribution, circulation persistence, and metabolism of functional ligands for medical applications.

This work was partly supported by MEXT, the Grant in Aid for Young Scientists (B) (No. 18740264), and by JSPS, the Grant in Aid for Scientific Research (B) (No. 16350093). T. S. acknowledges the 21st century COE program at Waseda University funded by MEXT. The authors appreciate the strong support of the late Professor Hironobu Kunieda for SAXS measurements and thank Professor Sow-Hsin Chen and Dr. Yun Liu for providing the MATLAB code for two Yukawa model [13].

*Email address: takaaki.sato@waseda.jp
†Email address: eishun@waseda.jp

[1] T. Peters, *All About Albumin: Biochemistry, Genetics, and Medical Applications* (Academic, New York, 1996).
[2] P. A. Zunszain *et al.*, BMC Struct. Biol. **3**, 6 (2003).
[3] X. M. He and D. C. Carter, Nature (London) **358**, 209 (1992).
[4] S. Curry *et al.*, Nat. Struct. Biol. **5**, 827 (1998).
[5] J. Ghuman *et al.*, J. Mol. Biol. **353**, 38 (2005).
[6] T. Komatsu *et al.*, Macromolecules **32**, 8388 (1999).
[7] T. Komatsu, Y. Matsukawa, and E. Tsuchida, Bioconjugate Chemistry **13**, 397 (2002).
[8] T. Komatsu *et al.*, J. Biomed. Mater. Res. **71A**, 644 (2004).
[9] T. Komatsu *et al.*, J. Am. Chem. Soc. **127**, 15 933 (2005).
[10] A. Tardieu *et al.*, J. Cryst. Growth **196**, 193 (1999).
[11] A. Stradner *et al.*, Nature (London) **432**, 492 (2004).
[12] Y. Liu *et al.*, Phys. Rev. Lett. **95**, 118102 (2005).
[13] Y. Liu, W. R. Chen, and S. H. Chen, J. Chem. Phys. **122**, 044507 (2005).
[14] M. Malfois, F. Bonnete, L. Belloni, and A. Tardieu, J. Chem. Phys. **105**, 3290 (1996).
[15] M. G. Noro, N. Kern, and D. Frenkel, Europhys. Lett. **48**, 332 (1999).
[16] T. Sato and R. Buchner, J. Phys. Chem. A **108**, 5007 (2004).
[17] G. Fritz, A. Bergmann, and O. Glatter, J. Chem. Phys. **113**, 9733 (2000).
[18] T. Fukasawa *et al.*, Phys. Rev. Lett. **95**, 197802 (2005).
[19] N. Nandi, K. Bhattacharyya, and B. Bagchi, Chem. Rev. **100**, 2013 (2000).
[20] Y. Hayashi *et al.*, Biophys. J. **79**, 1023 (2000).
[21] Y. Liu *et al.*, Phys. Rev. Lett. **96**, 219802 (2006).
[22] A. Stradner, F. Cardinaux, and P. Schurtenberger, Phys. Rev. Lett. **96**, 219801 (2006).
[23] F. Sciortino *et al.*, Phys. Rev. Lett. **93**, 055701 (2004).
[24] E. Bianchi *et al.*, Phys. Rev. Lett. **97**, 168301 (2006).
[25] V. Jeney, J. W. Eaton, and G. Balla *et al.*, Blood **100**, 879 (2002).
[26] E. Tolosano and F. Altruda, DNA and Cell Biology **21**, 297 (2002).